

2006 LLNL Nuclear Science Summer Internship Program

June 13 - August 11, 2006

Lawrence Livermore National Laboratory
Chemistry, Materials, and Life Sciences
Glenn T. Seaborg Institute
Livermore, CA 94550, USA

Web site: <http://cms.llnl.gov/review/seaborginstitute/index.html>

Director: Annie Kersting
Education Coordinator: Nancy Hutcheon
Administrative Assistant: Linda Jones



Sponsors:
Office of Nonproliferation Research and Engineering (NA-22)
Advanced Fuel Cycle Initiative
LLNL: Chemistry, Materials, & Life Science



The Lawrence Livermore National Laboratory (LLNL) Nuclear Science Summer Internship Program (NSSIP) is designed to give both undergraduate and graduate students an opportunity to come to LLNL for 8 weeks during the summer for a hands-on research experience. Each student conducts research under the supervision of a staff scientist, attends a weekly lecture series, interacts with other students, and presents their work in poster format at the end of the program. Students also have the opportunity to participate in LLNL facility tours (e.g. National Ignition Facility, Center of Accelerator Mass-spectrometry) to gain a better understanding of the multi-disciplinary science that is on-going at LLNL. A summer highlight is a weekend trip to Yosemite national park, where the students enjoy a weekend of hiking and socializing.

Currently called NSSIP, this program began eight years ago as the Actinide Summer Program. The program is run within the Glenn T. Seaborg Institute in the Chemistry, Materials, and Life Sciences Directorate at LLNL. The goal of NSSIP is to facilitate the training of the next generation of nuclear scientists and engineers to solve critical national security problems. We select students who are majoring in physics, chemistry, nuclear engineering, chemical engineering and environmental sciences. Students engage in research projects in the disciplines of actinide and radiochemistry, isotopic analysis, radiation detection, and nuclear engineering in order to strengthen the ‘pipeline’ for future scientific disciplines critical to NNSA.

This is a competitive program with over 170 applicants for the 15-20 slots available. Students come highly recommended from universities all over the country. For example, this year we had students from UC Berkeley, U Michigan, Stanford, Columbia University, Georgia Tech, UC Davis, Reed College, Middlebury and MIT. We advertise with mailers and email to all the nuclear science and chemistry departments in the U.S. We also host students for a day at LLNL who are participating in the D.O.E. sponsored “*Summer School in Nuclear Chemistry*” course held at San Jose State University.

This year students conducted research on such diverse topics as: cryogenic neutron spectrometers, nuclear forensics, cladding for advanced fission reactors, sorption of radionuclides, principal component analysis of spent reactor fuel, semiconductor detectors, actinide separations chemistry, and anti-neutrino monitoring of nuclear reactors.

Graduate students are invited to return for a second year at the mentor’s discretion. For the top graduate students in our program, we encourage the continuation of all collaborations between graduate student, faculty advisor and laboratory scientists. This creates a successful pipeline of top quality students from universities across the U.S. To date, 15 graduate students have continued to conduct their graduate research at LLNL. Three recent career hires were former summer students.

Seminar Schedule 2006

Wed June 21	Ken Moody, LLNL	<i>"Nuclear Forensics"</i>
Wed June 28	Mike Pivovarov, LLNL,	<i>"From High Energy Astrophysics to Homeland Security - Making the Link"</i>
Thur June 29	Armando Alcaraz, LLNL	<i>"Forensics Sciences and national security at LLNL"</i>
Wed July 5	Rick Ryerson, LLNL	<i>"Raising Tibet"</i>
Thur July 6	John Perkins, LLNL	<i>"Fusion, the Ultimate Energy Source"</i>
Tues July 11	Mike Carter, LLNL	<i>"Countering Nuclear Terrorism - A Grand Challenge in Homeland Security"</i>
Thurs July 13	Ed Moses, LLNL	<i>"NIF, The National Ignition Facility"</i>
Wed July 19	Bob Criss, Washington University	<i>"Earth's Radioactivity, Heat Flow and Convection"</i>
Thur July 20	Bob Maxwell, LLNL	<i>"Nuclear Magnetic Resonance Center"</i>
Tues July 25	Eric Gard, LLNL	<i>"Bio-Aerosol Mass Spectrometry"</i>
Thur July 27	Alex Hamza, LLNL	<i>"Nanomaterials Synthesis and Characterization"</i>
Wed Aug 2	Glenn Knoll, University of Michigan	<i>"Fundamentals of Radiation Detection"</i>
Thur Aug 3	Jim Rathkopf, LLNL	<i>"Principles of Nuclear Weapons Physics"</i>
Thur Aug 10	Jon Maienschien, LLNL	<i>"High Explosives Research"</i>

Summer Students 2006

<u>Student</u>	<u>Major</u>	<u>University</u>	<u>Year</u>
Amy Coffey	Nuclear Engineering	U Michigan	Undergrad
Bhushar Mookerji	Physics/Electrical Engineering	MIT	Undergrad
Elaine Hart	Materials Science	Stanford	Graduate
Daniel Heineck	Electrical Engineering	Oregon State University	Graduate
Greg Brennecka	Nuclear Chemistry	U Rochester	Graduate
Jeremy Waen	Chemistry	Reed College	Graduate
John Clements	Environmental Engineering	Clemson	Graduate
Kevin Stein	Physics	UC Berkeley	Undergrad
Martin Robel	Nuclear Engineering	UC Berkeley	Graduate
Paul Koster van Groos	Environmental Engineering	UC Berkeley	Graduate
Rion Graham	Physics	UCLA	Undergrad
Tsuguo Aramaki	Physics	Columbia	Graduate
William Coleman	Physics	LSU	Graduate
Shadi Ghayeb	Nuclear Engineering	Rensselaer Polytechnic Institute	Undergrad
Alex Johnson	Nuclear Engineering	Georgia Tech	Undergrad
Nathanael Kuo	Electrical Engineering	U of Illinois	Undergrad
Benjamin Westbrook	Physics	U San Francisco	Undergrad
Ryan Till	Mechanical Engineering	U Arizona	Undergrad
Megan Brinkmeyer	Chemistry	St. Mary's College	Undergrad



Unfolding a Cryogenic Neutron Spectrometer

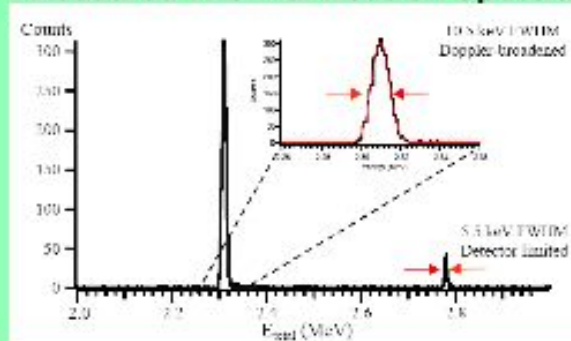


Amy Coffey, Nuclear Science Summer Internship Program
Thomas Niedermayr, I-Div, Physics and Advanced Technologies

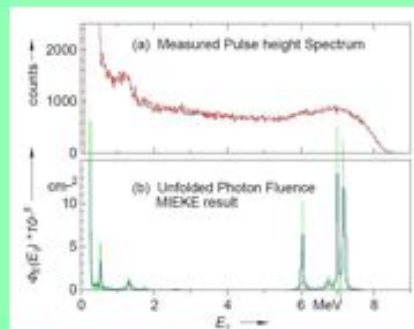
The Detector

- Nuclear Attribution
- Microcalorimetry
- High Resolution ~ 0.1%
- Compact and Commercially Available

Measured Thermal Neutron Spectra



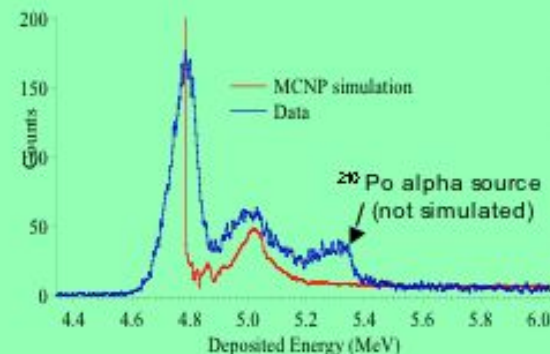
Unfolding



Example of unfolding a low resolution detector

- Increase System Performance
- Know Detector Response
- Mathematical Technique
- More Accurate and Precise Info

Simulation



MCNP simulation matches detector measurement

- Quality of Unfolding
- MCNP
- Maximum Entropy
- PTB Computer Code



Glenn T. Seaborg Institute

The optical constants of Gallium stabilized d-phase plutonium metal between 0.7 and 4.3 eV measured by spectroscopic ellipsometry using a double-windowed experimental chamber

Bhaskar Mookerji^{1,2} and Wigbert J. Siekhaus³

¹Undergraduate Summer Institute ²Massachusetts Institute of Technology; Cambridge, MA 02139

³Material Science and Technology Division, Chemistry and Material Science Directorate, LLNL; Livermore, CA 94550

Abstract

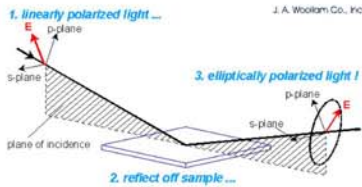
A double-windowed vacuum-tight experimental chamber was developed, and calibrated on the spectroscopic ellipsometer over the energy range from 0.7 to 4.5 eV using a silicon wafer with approximately 25 nm oxide thickness to remove the multiple-window effects from measurements. The ellipsometric measurements were done such that incident and exit beam were at 65 degree from surface normal. The plutonium sample (3 mm diameter, 0.1 mm thick) was electro-polished and mounted into the sample chamber in a glove box having a nitrogen atmosphere with less than 100ppm moisture and oxygen content. The index of refraction n and the extinction coefficient k decrease from 3.7 to 1 and 5.5 to 1.1 respectively as the photon energy increases from 0.7 to 4.3 eV.

Introduction

The optical constants (n and k , coefficients of refraction and extinction, respectively) of plutonium metal are of scientific and practical interest, but not readily available. They are difficult to measure, because only small quantities can be handled since the material is highly radioactive. Moreover, safety regulations require that plutonium be doubly contained at all times.

To accurately measure these properties, we first design a double-windowed experimental cell that secures a plutonium sample. A variable angle spectroscopic ellipsometer (J.A. Woollam Co., In. Lincoln, Nebraska 68508) will then be calibrated to apply numerical corrections at measurement-time to account for systematic errors introduced by doubled Pyrex windows. A pre-existing bulk metal model can then be applied to model our plutonium data once it has been taken.

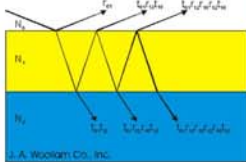
Introduction to Ellipsometry



$$\rho = \tan(\psi) e^{i\Delta} = \frac{\tilde{R}_p}{\tilde{R}_s}$$

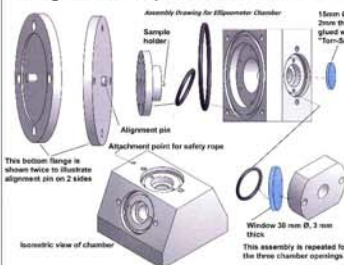
Ellipsometry measures two parameters, ψ and Δ , which are related to Fresnel reflection coefficients. An infinite, convergent series of transmitted and reflected light sums to these coefficients.

Ellipsometry uses polarized light to characterize thin films and surfaces. Incident light interacts with the sample, changing from a linear polarization state to an elliptical polarization state. This polarization change is determined by measuring the light reflected from the sample.



Experimental Methods and Analysis

Design of the Experimental Chamber



The experimental chamber holds the Pu sample in two separate enclosures and ensures its precise and reproducible alignment on the ellipsometer's working platform. The doubled Pyrex windows exposes 3mm wide samples to light incident at 65 degrees relative to the sample's surface normal vector.

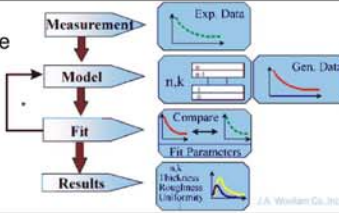
Sample Preparation and Window Calibration

The Pu sample was mechanically and electrochemically polished in a moisture-free, N₂ glove-box. The sample was approximately 101 μm thick and 3mm in diameter. Transmission electron microscopy on similar samples indicated an oxide thickness of a few nm.

Before the Pu measurement, a silicon wafer standard (3mm Ø with a 25 nm thick SiO₂ layer) was cleaned in air using acetone and was then mounted horizontally in the bottom of the ellipsometer cell. The cell and silicon wafer were then mounted vertically in the ellipsometer, during which a software calibration script determines a "window effect correction function" that is used to correct Δ and Ψ data from unknown samples in the chamber.

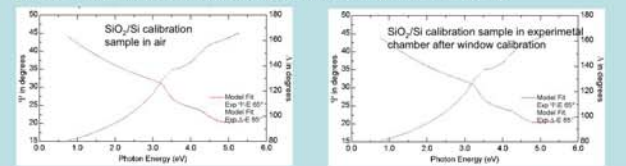
Ellipsometry analysis procedure

Following measurement, the Pu sample is modeled as bulk metal sample using initial data provided for well-polished, bulk gold. The model's generated constants are adjusted until they fit the experimental data.



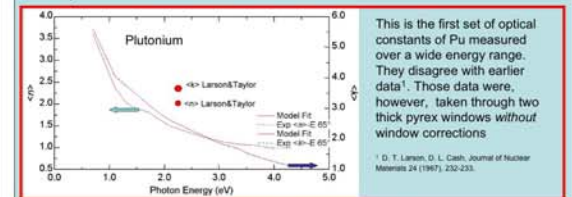
Results and Discussion

Window Calibration Procedure Eliminates Window Effects



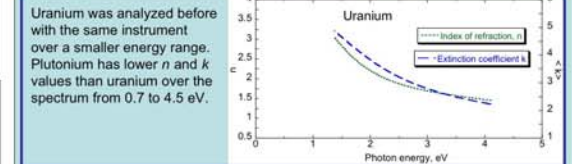
The two figures show experimental data taken from a 1cm² oxidized Si wafer mounted first in air, and then in the experimental cell. A model consisting of bulk silicon, a 1 nm thick Si/SiO₂ interface layer and a SiO₂ layer of adjustable thickness was applied. In the cell, the measured oxide thickness (25.808 +/- 0.018 nm) did not differ significantly from the given value of 25.000 nm. The sample in open air measured 25.484 +/- 0.0456 nm.

Optical Constants: Plutonium and Uranium



This is the first set of optical constants of Pu measured over a wide energy range. They disagree with earlier data¹. Those data were, however, taken through two thick pyrex windows without window corrections

¹ D. T. Larson, G. L. Cash, Journal of Nuclear Materials 24 (1967), 432-433.



Uranium was analyzed before with the same instrument over a smaller energy range. Plutonium has lower n and k values than uranium over the spectrum from 0.7 to 4.5 eV.

Conclusions

- We have demonstrated the reliability of a window calibration procedure for double-window experimental chambers that are needed for optical analysis of transuranium elements
- We have used it to determine the unknown optical constants of Pu metal.
- With this new data we can extend our procedure to determining the optical constants of plutonium surface oxides, part of a larger project to fully characterize the optical properties of plutonium.

Acknowledgments

This work was performed under the auspices of the U. S. Department of Energy by the University of California, Lawrence Livermore National Laboratory under Contract No. W-7405-Eng-48. The Seaborg Institute at LLNL supported B. Mookerji. We gratefully acknowledge the support of Gerry Cooney and James Hilfinger of J.A. Woollam Co. Inc. for software support. Special thanks to Martin Stratman for design/machining of the experimental cell and Mark Wall for handling the the plutonium samples.



A Field Ionization and Ion Acceleration Model for a Novel Pyroelectric Crystal-Based Neutron Source

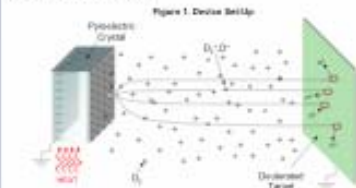


Glenn T. Seaborg Institute

Elaine K. Hart, Nuclear Science Summer Internship Program
 Jeff Morse, Ben Fasenfest, Chris Spadaccini
 Center for Micro- and Nanotechnology, LLNL

Background: Pyroelectric Crystal Ion Acceleration

Pyroelectric crystals like lithium tantalate are known to produce electric fields upon heating or cooling. This phenomenon has been utilized in the past to create small x-ray emitters by concentrating the electric field with a small metal pin attached to a metal plate that lies on the surface of the crystal. Concentrated electric fields from pyroelectric crystals have more recently been used in small neutron sources, with varied success.¹ The system is shown in Figure 1.



In regions near the metal tip, the electric field is strong enough to ionize ambient deuterium molecules and accelerate the products to the deuterated or tritiated target. Upon collision, the high energy accelerated deuterons and the deuterons in the target undergo nuclear fusion and emit a neutron. Recent experiments at UCLA have produced up to 4nA of ion current from such experiments.² The goal of this research was to model the gas phase field ionization and acceleration process in order to optimize the experimental parameters for producing high ion currents.

Self-Consistent System Model

The self-consistent system model calculates the surface charge, surface potential, and ion current provided the physical parameters of the device and the temperature ramping function. The model assumes that the surface charge changes due to three processes: accumulation via the pyroelectric effect, loss due to ionization of deuterium, and loss due to leakage back through the crystal.

$$dQ_{tot} = dQ_{pyro} + dQ_{ion} + dQ_{leak}$$

$$dQ_{pyro} = p \cdot dT \cdot A$$

$$dQ_{ion} = -I_{ion} dt$$

$$dQ_{leak} = -\frac{Q_{tot}}{R} dt$$

Charge accumulation due to the pyroelectric effect depends only on the pyroelectric properties of the crystal and the temperature ramping function. The leakage loss can be approximated based on experimental reality data for lithium tantalate.³ The calculation of the ion current, however, is rather complex and requires the incorporation of a separate ionization model. Ionization was modeled using both a closed form model and a Monte Carlo simulation, which are described at right.

The surface potential is calculated based on the surface charge, assuming that the crystal acts as a capacitor.

$$V = \frac{Q_{tot}}{C}$$

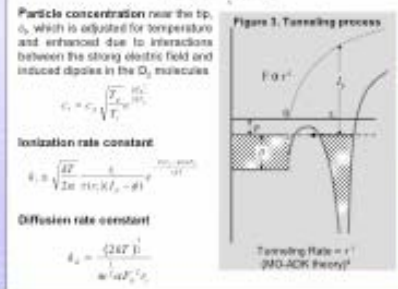
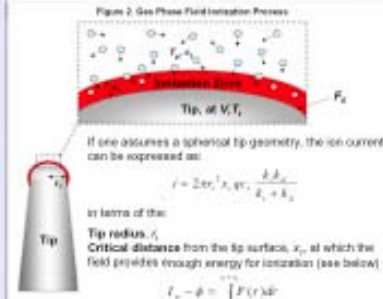
$$C = A \left(\frac{\epsilon_0}{d} + \frac{\epsilon_c}{d_c} \right) \approx A \frac{\epsilon_c}{d_c}$$

Note that the surface potential is also an input for the ion current calculation, as it determines the size of the high field region surrounding the tip. Self-consistency is assumed by recalculating the surface charge and surface potential until they are unchanged to within 0.1%.

A new portable neutron source utilizes the electric field produced by heating a pyroelectric crystal to ionize deuterium and accelerate the ionized species to a deuterated or tritiated target. This process is thought to produce neutrons via nuclear fusion at the target. A system model has been developed to describe this process and to optimize the design of the device. Separate sub-models were developed to describe the charge accumulation on the surface of the crystal due to the pyroelectric effect, field concentration by a metal pin and to afford to the crystal, field ionization due to these concentrated fields, and ion acceleration under these fields. The system model incorporates these sub-models in a self-consistent fashion and allows for the adjustment of several device parameters, including the input temperature ramping function, the deuterium pressure, the pyroelectric coefficient and dimensions of the crystal, and the metal tip geometry. Early results suggest that enlarging the tip has little impact at high temperature ramp rates and that achieving high ramp rates may provide ion currents an order of magnitude higher than previously observed in experiment.

Closed Form Gas Phase Field Ionization Model

A field ionization model commonly used for Gas Field Ionization Sources (GFIS) was used to determine the functional relationship between the surface potential and the ion current.⁴ In this model, ionization rates depend on the rate in which particles enter the ionization zone around the tip, the time each particle spends in the ionization zone, and the probability of ionizing within this zone.



Monte Carlo Field Ionization Simulation

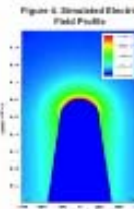
The closed form field ionization model predicts field ionization will for GFIS devices that typically operate at very low temperatures, but it may not fully incorporate the effects of thermal molecular velocities. To achieve this, a Monte Carlo simulation was developed. The Monte Carlo field ionization model constructs a box around the tungsten tip filled with deuterium molecules each traveling in a random direction at a fixed initial speed based on the Maxwell-Boltzmann distribution. The electric field induces a dipole in each deuterium molecule according to:

$$\mu = \alpha D_2$$

where α is the polarizability of D_2 . The molecules are assumed to align in the electric field so that the force on each molecule from the field is:

$$F = \nabla E \cdot \mu = \alpha \nabla E^2$$

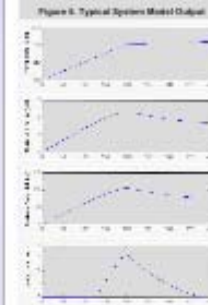
This dipole force is calculated for each molecule by approximating the electric field strength and gradient at the molecular positions. The electric field (shown at right for a 0.1 micron radius tip) was calculated using COMSOL, a parallel finite element solver. The effects of the dipole force on a deuterium molecule can be seen in Figure 5.



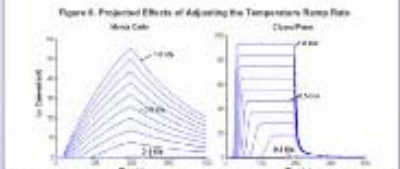
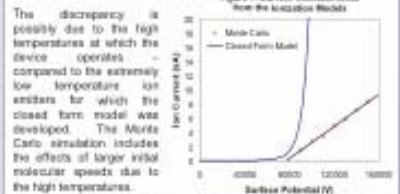
Ionization events are currently simulated by the annihilation of molecules that enter regions of high electric field strength ($> 25V/nm$). Further development of the model will incorporate a field-dependent ionization probability function. The Monte Carlo simulation records the average time between ionization events in order to calculate the ion current.

Results and Conclusions

An example of the system model output is shown in Figure 6. The most recent results indicate that the Monte Carlo simulation differs from the closed form model and may better replicate experimental data.



The current characteristics from the two ionization models are shown in Figure 7. The closed form model predicts a steep increase in current as a function of voltage above a threshold voltage of approximately 80kV. The Monte Carlo simulation was less successful at modeling the low field regime, but predicts a more gradual current curve above the threshold surface voltage. As a result of the different current slopes, the two ionization models provide two completely different pictures of the device's behavior at high temperature ramp rates. This is illustrated in Figure 8.



Development of an ion acceleration model to accompany the Monte Carlo system is currently underway. The ion acceleration model is being designed to calculate the trajectories and energies of the ionization products and has the aim of reorienting the neutron output at the device target.

References

1. D. Narango, J.K. Grossnickel, and S. Robertson, *Nature* 434, 1115-1117 (2005).
2. S. Lang and Y. Yu, *Phys. Scr.* 331, 421-429 (1994).
3. Gomer, Robert, *Field Emission and Field Ionization*, Harvard University Press, 1981.
4. X.M. Tong, Z.X. Zhou, and C.D. Lin, *Phys. Rev. A*, 48, 5332-5337 (2003).

This work was performed under the auspices of the U.S. Department of Energy by the University of California Lawrence Livermore National Laboratory under contract No. W-7409-Eng-02.



Glenn T. Seaborg Institute

Pillar-Based Neutron Detector

Daniel Heineck, Nuclear Science Summer Internship Program

Rebecca Nikolic, Catherine Reinhardt, EETD
Lawrence Livermore National Laboratory



This part of the pillar-based neutron detector project aims to find a reliable ohmic contact process with the goal of a specific contact resistance of $10^{-4} \text{ } \Omega\text{-cm}^2$ for both sides of the detector. For the P+ side, Aluminum, layered Ni/Ti/Au, Pd/Ti/Au, and Pt/Ti/Au schemes are tested at multiple annealing temperatures. For the N+ side, Aluminum and a layered Ti/Pt/Au are examined. The Pt/Ti/Au metal scheme proves to be the most effective contact method for the P+ side, whereas the N+ contact design is not yet determined. The Pt/Ti/Au contact with a 3.5 minute anneal at 300°C has a specific contact resistance of $6.6 \times 10^{-4} \text{ } \Omega\text{-cm}^2$.

Introduction:

- Boron 10 absorbs incident neutrons, releasing a ^7Li and an α particle in opposite directions
- The energetic ions then collide with silicon atoms in the pillars, exciting the outer shell electrons out of their lattice sites.
- High electric field accelerate electrons to the positive terminal of the device
- Pillar design is chosen in order to maximize the number of ion collisions in the silicon
- Low resistance ($10^{-4} \text{ } \Omega\text{-cm}^2$), low leakage electrical contacts are critical to ensure maximum signal to noise ratio for the detector

Work Function (ϕ) is the energy difference between E_v and E_f

N-Type Silicon ϕ_{Si} 4.12 eV
P-Type Silicon ϕ_{Si} 5.08 eV

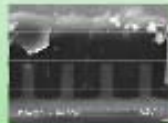
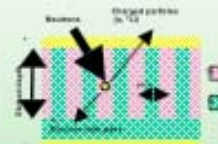
Metal Work Functions

Aluminum 4.28 eV
Titanium 4.55 eV
Palladium 5.12 eV
Nickel 5.15 eV
Platinum 5.65 eV

N+ Metal Scheme $\phi_{\text{Si}} > \phi_{\text{M}}$
P+ Metal Scheme $\phi_{\text{Si}} < \phi_{\text{M}}$



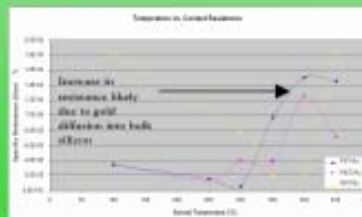
As shown on n-type material, electrons tunneling through the potential barrier are field emissions. Ohmic contacts are designed to fit this category. Electrons that have sufficient kinetic energy to pass over the barrier are thermionic emissions.



Pillar structures after boron 10 has been deposited in the gaps. The CVD process development is done by Barry Cheng, University of Nebraska. Samples are then lapped and polished back to the pillar height.

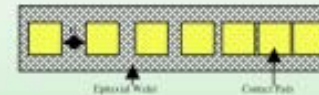
Results:

The Platinum/Titanium/Gold metal scheme has the lowest R_c of all the front side metal schemes chosen since it has a low eutectic temperature with silicon and has the highest work function, which reduces the potential barrier between the metal and the semiconductor. This value is only $6.6 \times 10^{-4} \text{ } \Omega\text{-cm}^2$ when the sample is annealed at 300°C for 3.5 minutes. Palladium and nickel base layers also show promise and their processes will be further examined.

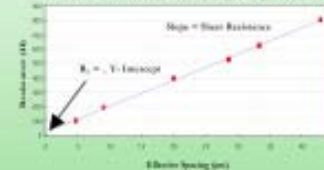


Method:

1. Mask small epitaxial samples with a lift-off photoresist pattern
2. Deposit metal schemes onto epitaxial samples using E-beam evaporation
3. Characterize specific contact resistance (R_c) by measuring the transmission line method (TLM) structures on samples before sintering process
4. Measure R_c for sintering temperatures ranging from 250°C to 450°C for 30 seconds
5. Vary anneal time for each scheme at respective optimal temperature.



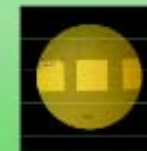
The transmission line method (TLM) structure.



Distance vs. resistance graph used to calculate R_c



Right and left are a Pt/Ti/Au contact after a 300°C, 3.5 minute anneal and a Ni/Ti/Au contact after a 375°C 30 second anneal. The edges of the nickel sample show gold diffusion into the titanium, whereas the lower temperature platinum sample does not.



Discussion:

In order to reduce the specific contact resistance by an order of magnitude, variations in the thickness of the current Pt/Ti/Au layers will be examined. To complete the crystallization of the PtSi_2 silicide, longer anneal times will be examined. Once the goal contact resistance is met, an X-ray diffraction analysis of the surface chemistry will occur. Typically, N+ silicon and aluminum make excellent contacts at very low (200-350°C) sintering temperatures. However, the N+ back side contacts are still a work in progress. Once the ohmic contact process is completed, a basic electrical model of the sensor will be developed.



Applications of Mass Spectrometry in Nuclear Forensics

Greg Brennecka - University of Rochester (NSSIP student)

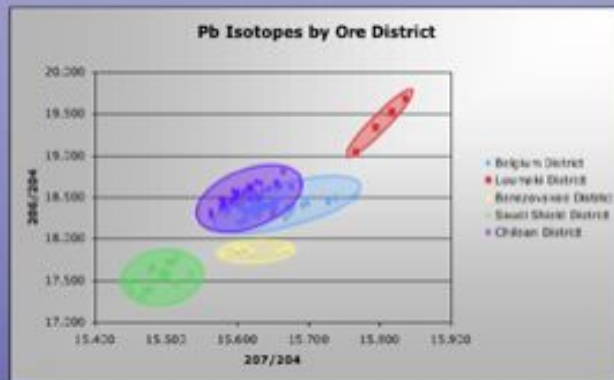
Erick Ramon - Chemical Biology and Nuclear Science Division, CMS



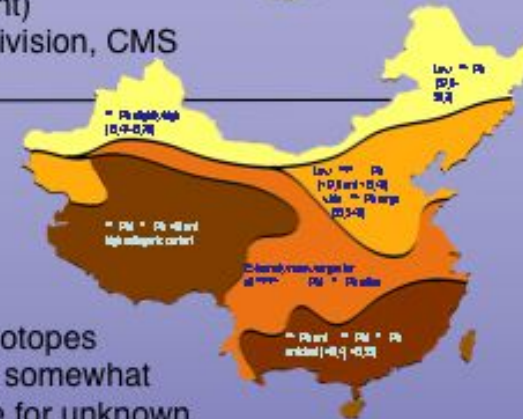
Glenn T. Seaborg Institute



Geolocation using a Pb isotope database

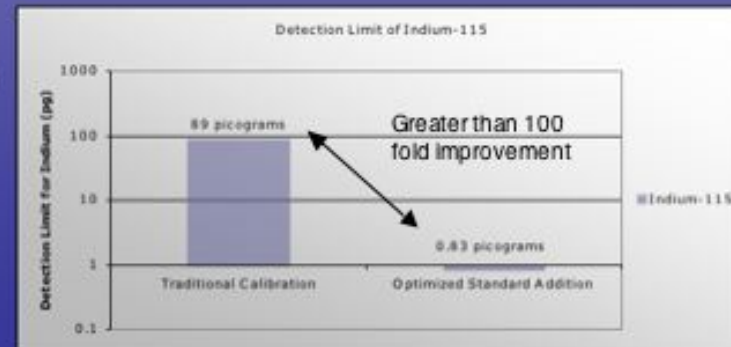


Natural variance of Pb isotopes worldwide can provide a somewhat unique isotopic signature for unknown samples containing Pb (less than 5 ppb)



Improved analytical capability for characterizing elemental impurities in uranium oxide

- Uranium oxides contain elemental impurities that can be used to determine provenance and handling procedures.
- Signal suppression from a high uranium matrix reduces our ability to accurately measure trace element impurities.
- A new technique was developed which reduces signal suppression and improves data quality.





Sorption Studies of Eu and Cs with Urban Surfaces i.e. How to Clean Up the Worst of Messes

Jeremy G. Waen, Nuclear Science Summer Internship Program

Mark Sutton, CBND, CMS, Bob Fischer, RHWM, SEP, Brian Viani, Geochemistry, E&E

August 10th, 2006



Glenn T. Seaborg Institute



Reed College

Abstract

In the aftermath of September 11 events the concern for national security has heightened. Among the numerous weapons available to terrorists are Radioactive Dispersal Devices (RDDs). While many steps are being taken to prevent smuggling of such weapons across our borders, very little research has been carried out addressing how such an attack could be contained and decontaminated. A team of scientists at the Lawrence Livermore National Laboratory (LLNL) is collaborating to address this issue. Urban surface samples have been collected in from major transit locations. The used structural and chemical compositions of these materials are being studied along with how they interact with radionuclides used for RDDs. In the near future experiments sorption and desorption

ions were exposed to surface grime taken from an urban site. The quantity of grime and the pH (4 or 10) were varied in order to observe different possible sorption interactions. Results were fit to linear, Langmuir, Freundlich, and Freundlich plus linear adsorption. Out of the four sets of solutions only the alkaline sorption solutions showed any evidence of sorption interactions between the Eu ions and the surface grime. Since sorption acts as a chemical analogue to an adsorbate, these results will help their scientific design cleanup and containment methods of Air-based RDDs.

The Issue:

Terrorist-Dispersed Radionuclides



The Chemistry Behind The Threat

The true threat that RDDs pose is not a matter of devastation but a matter of disruption. Even if the actual amount of explosive used is small, if detonated in the proper location an RDD can spread radionuclides over vast areas. In addition because of the general public's longstanding fear of nuclear technology, panic and economic disaster could easily result. Estimates show the economic impact of the detonation of an RDD would be on the magnitude of billions of dollars. A full recovery would take months, even years. For three reasons, the reason for a well organized response to decontaminate an RDD explosion are in dire need. Because RDDs locally act as a chemical threat, a strong understanding of possible chemical environments is necessary.

Furthermore the chemistry governing how radionuclides might interact with these environments must play a crucial role in determining how to approach the issue of decontamination. The three primary objectives for this team's research are:

- To Characterize Urban Surface Materials & Understand How These Surfaces Weather
- To Study Sorption Of Radionuclides With These Materials & To Accurately Simulate Explosive Dispersion
- To Design Chelators To Leach Out Radionuclides & To Optimize Chemical Delivery and Cleanup Techniques

A Plethora Of Samples

Samples were collected at three different locations across the country. All three locations are similar because they are all situated in heavily urban environments around central transportation points. Any of these locations would be ideal settings for a radioactive terrorist. Numerous samples were collected at each of these three locations. Some samples were composed of concrete while others were primary walls of steel or other types of materials used in construction. Samples were selected from various different surfaces: walls, floors, ceilings, and windows. Furthermore the samples were collected in a number of different ways. In some cases the vacuum was used to lift samples off surfaces. In other cases spools with different solvents were used to pick up layers of grime.



Core samples were drilled out of concrete so that the different layers of material could be studied in an undisturbed state. In some cases these different sublayers were used to collect samples in the same location, that way the effectiveness of each cleaning technique could be evaluated carefully.

The Approach: Analyzing the Environment



Looking Below The Surface

By studying the collected core samples it was discovered that there are three fundamental layers to the surface of aged urban concrete. The outer most layer is a thin layer of grime. Powdered debris composed of concrete dust, rusted metal scraps, and whatever else might collect over time. Below this is a layer of concrete that has been weathered and neutralized. This region has a lower pH than the bottom layer of normal concrete. Due to these three chemically distinct layers, it is believed that radionuclides will have different interactions depending upon their depth. A heavy explosive test at site 100 was used to study the depth that these particles could penetrate due to a RDD explosion.

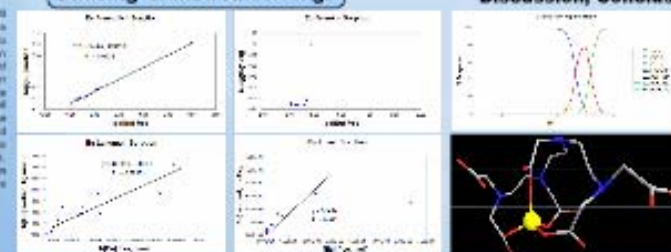


Sorption Studies Of Radionuclide Analogs

Another way to study how well radionuclides will stick to these different types of through sorption studies. Known amounts of grime were used with known amounts of ions at a fixed pH. Both cesium and europium ions were used as radionuclide analogs. The solutions used pH 4 and 10 buffers as shown. The results parameter was the amount of grime which ranged from 0.020 g to 0.200 g. 10 mL samples of ions solution were mixed with portions of grime, shaken for a week, filter, and then filtered before being subjected for analysis. Upon releasing the results, it was found that only the alkaline sorption gave evidence signs of cesium sorption relative to the concentration of grime present. The results from the analysis of the Cs pH 10 samples were then fit to different types of plots. The linear plot demonstrated a constant of sorption of 3248 cc/g. The Langmuir plot tells us that the maximum adsorption capacity was 3.48E5 Bq/g. Finally, the Freundlich plot yields a non-linearly function of 5.62E6. This confirms our belief that the grime layer has a

chemically heterogeneous surface if this value were 1.0E the grime would be considered homogeneous. The Freundlich plot indicates inductive results. The plot is used to determine the presence of binding interactions between Eu species. Further study through NMR is needed to explain what interactions might be happening between neighboring Eu ions and their ligands. The result from the Freundlich plot is especially insightful because it fits well with previous elemental analysis done on similar grime samples. Through XRF, total acid digestion, XPS, and other techniques it has been discovered that this surface grime is primarily composed of wet oxides and silicates. Thus it is believed that most of the sorption interactions occur between the Eu species and the oxides of these chemical species.

The Solution: Utilizing Gained Knowledge



Discussion, Conclusions, & Future Plans

The successful sorption of only the alkaline Eu sample can be explained by this as well. Most non-oxide material positively charged surfaces in environments below ~7 pH. Above this same pH these surfaces are negatively charged. Computer modeling shows us that Cs will primarily form a Cs^{2+} cation in acidic solution, but it will form a $CsCO_3^{+}$ cation in basic solution. Strong separation of like charges explains why the pH 4 samples did not react. The pH 10 reactivity is due to the bulky hydroxide component of the anion and the attraction between the negative oxygen of the grime and the positive metal. Both cesium samples showed no evidence of sorption, but this is not terribly surprising because Cs is known to be difficult to bind. Sorption acts as an analogy for americium, which is a likely radionuclide for RDDs. Therefore the results of the experiment suggest that an acidic wash would help to lift Am ions from urban surfaces. The next major step in this groups research is to design chelating agents and cleaning techniques for the decontamination of terrorist RDDs.



Optimization of Ion-Exchange Separations of Neptunium, Plutonium, and Uranium in Groundwater Samples from the Nevada Test Site

John P. Clements, Nuclear Science Summer Internship Program
Mavrik Zavarin, Pihong Zhao, Chemistry & Material Science



Glenn T. Seaborg Institute



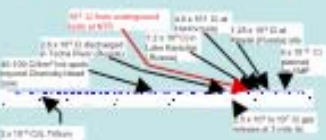
Recent reactive transport model simulations of the Cantons Underground nuclear test have predicted Np concentrations at these wells (RMA-1, RMA-25, and UE-5a) that are inconsistent with reported Np concentrations at those sites. To resolve this discrepancy, we have improved our detection limits and optimized our procedures for Np, Pu, and U separation from Nevada Test Site (NTS) groundwater. Np preconcentration and separation was performed on groundwater samples from the three wells of interest (RMA-1, RMA-25, and UE-5a). Np preconcentration from 10 liter groundwater samples was performed using MnO_2 and $Fe(OH)_3$ as oxidizable scavengers. The MnO_2 precipitates were dissolved in concentrated HNO_3/HF acid, redissolved into a $3M HNO_3/0.22M NH_4OH/HClO_4$ (M-Pe) solution, and loaded onto Eichrom TEVA resin columns. The Hydroxylamine HCl is able to reduce Pu to Pu(II), while leaving U as U(VI), and reducing Np(V) to Np(IV), Np(V) is favorable to TEVA column sorption. $3M HNO_3$ effectively removed Pu(II) and U(VI) from the column. Np elution was accomplished with $0.02M HCl + 0.2M HF$. Samples are analyzed ICP-MS analysis, based on ^{237}Np gamma counting. $>90\%$ recovery has been achieved.

Introduction

The Underground Test Area Project is evaluating radionuclide contamination at the NTS.



Method for groundwater separation



Process: Concentration is distributed over a polymeric ion exchange resin, followed by elution of only one.

Separation of actinides from groundwater



Recent data indicate that Np may be present at RMA-1, RMA-25, and UE-5a. Relative transport models suggest little or no Np transport to UE-5a. We are attempting to resolve this discrepancy.

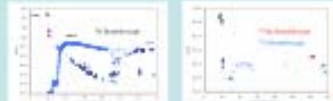
Methods

Preconcentration:

- We considered preconcentration based on current LANL and LLNL procedures:
 - Manganese oxide
 - Iron oxide
- MnO_2 was chosen for preconcentration and the following were investigated:
 - How much MnO_2 is required to quantitatively scavenge Np from 10 L groundwater samples collected from NTS wells?
 - Is the addition of $Fe(III)$ into the solution beneficial to Np scavenging?

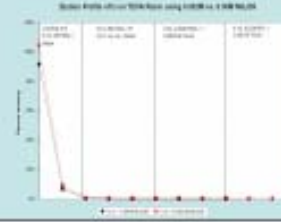
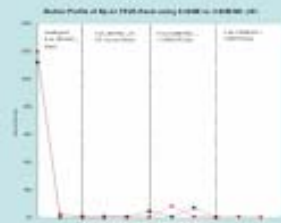
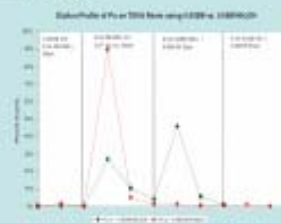
Column Separation:

- Np separation effectiveness was investigated:
 - What oxidation or reduction chemistry is required to effectively separate Np in NTS type groundwater matrices? (Hydroxylamine concentrations needed for reducing Np(V) to Np(IV) and what effect it has on Pu)
 - What role does $Fe(II)$ play in Np(V) reduction to Np(IV) and to the final separation on the TEVA column?
 - Can ^{237}Np (3-2 days) be effectively used to calculate ^{239}Np recovery from groundwater?
- Optimized column separation:
 - Loading in a $3M HNO_3/0.22M NH_4OH/0.02M Fe(II)$ solution.
 - Wash with $3M HNO_3$ to remove U and Pu.
 - Elute Np with $0.02M HCl + 0.2M HF$.



The study details in (RMA-1) (RMA-25) and (UE-5a) have been used to evaluate the model. Reduced concentration of washing solutions used to evaluate transport model parameters. Np removed at RMA-25 and UE-5a for waste purification.

Results



Discussion/Conclusions

- The addition of Fe into solution appears to be necessary for Np reduction/separation.
 - $0.02M NH_4OH$, 9.0%
 - $0.06M NH_4OH$, 5.1%
 - $0.22M NH_4OH/0.02M Fe(II)$, $>60\%$
- A relatively high NH_4OH concentration is required for effective Pu and Np reduction ($> 0.1M$ and preferably $0.22-0.33M$)
- Uranium (which is a major interference to ICP analysis of Np) can be effectively removed in 8-10 bed volumes of $3M HNO_3$.
- Excess $NaNO_2$ is required to effectively oxidize Pu(III) to Pu(IV), if it is desirable to sorb Pu to the TEVA resin. The nitrite must be sufficient to destroy all hydroxylamine in solution as well as oxidize Pu.
- At least $0.2M HF$ is needed to effectively remove Np from the column
- Final methods for NTS groundwater samples achieved $\sim 55\%$ Np recovery using ^{239}Np tracer
- ^{237}Np analysis is underway



LSST - The Next Level of Ground-Based Detection



Kevin Stein, Nuclear Science Summer Internship Program
Stephen Asztalos, I-Division, Physics and Advanced Technology
Lawrence Livermore National Laboratories
August 10, 2006



The Project

The Large Synoptic Survey Telescope (LSST) is a proposed telescope that will help astronomers solve certain cosmological problems. LSST, with its 8.4 meter diameter, will have a resolution of 0.146 arc seconds and a field of view of three square degrees. It will be able to detect a 24th magnitude star with only a ten second exposure. These specifications will allow astronomers to indirectly search for dark matter and observe distant supernovae that give clues to the shape of the universe. LSST is projected to be completed in 2012. Simulations were needed to examine how an industry standard detection program, Source Extractor, would respond to LSST images and what corrections would have to be made to obtain correct data.

Methods

- Using a randomly generated list of stars, a simulation of an LSST image was created using a program named Sky Maker.
- This image was then convolved with an atmospheric point-spread function (PSF). At first this PSF was manually created but later the program Arroyo was used to create a sophisticated PSF.
- The sources in the convolved image were extracted using Source Extractor.
- The brightnesses (magnitudes) and the ellipticities of the extracted stars were compared to the input data.



Figure 1: Planned site for LSST

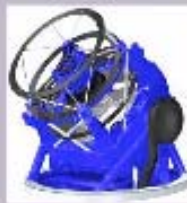


Figure 2: LSST Design



Figure 3: Initial image



Figure 4: Arroyo PSF



Figure 5: Convolved image

Discussion

The results of all of these simulations show astronomers how to correct the data that they will get from LSST. The analysis shows that astronomers won't have a problem making the ground-breaking observations that LSST is being built to make.

Results

- As magnitude increases, systematic error in detection increases.
- Worse seeing (higher FWHM) adds to the systematic error
- Added ellipticity doesn't have as much of an effect.
- Source ellipticity is expected to be dependent on the length of the exposure



Figure 8: Drawing of LSST in use



Figure 7: Pretty simulated image

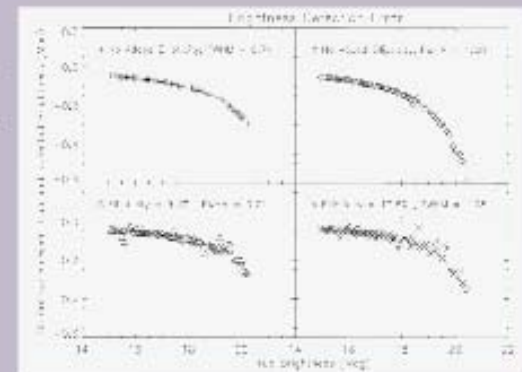


Figure 6: Results of initial simulations

Characterization of Spent Reactor Fuel Using Principle Components Analysis



Martin Robel

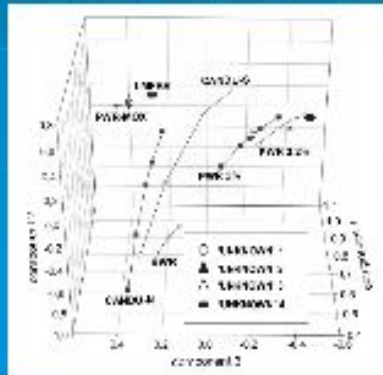
University of California, Berkeley, Department of Nuclear Engineering

Lawrence Livermore National Laboratory Nuclear Science Summer Internship Program

Mentor: Mike Kristo, C&MS Division

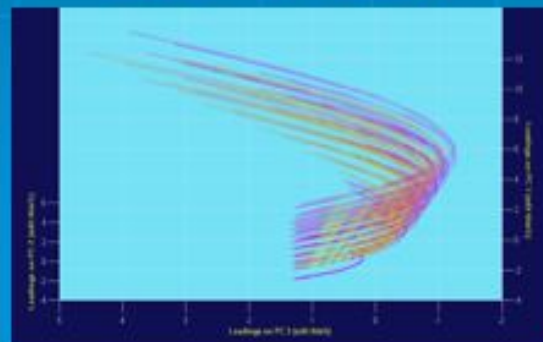


Idealized



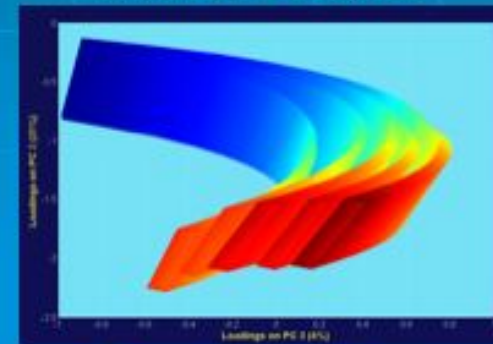
Note clear separation

Closer to Reality

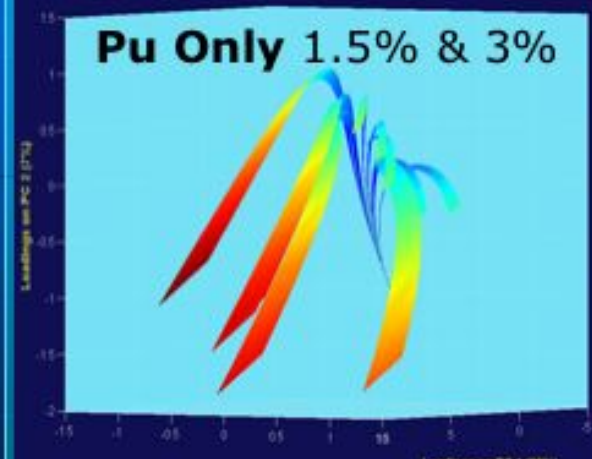
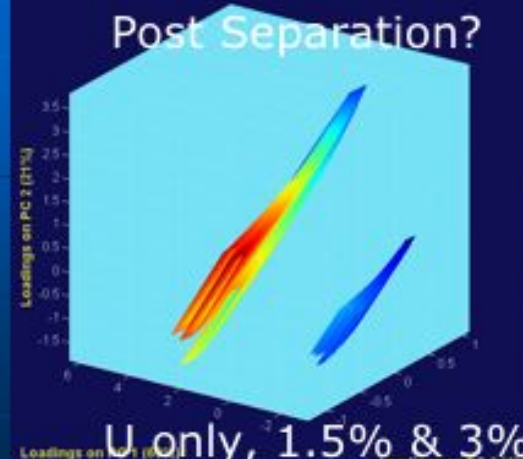
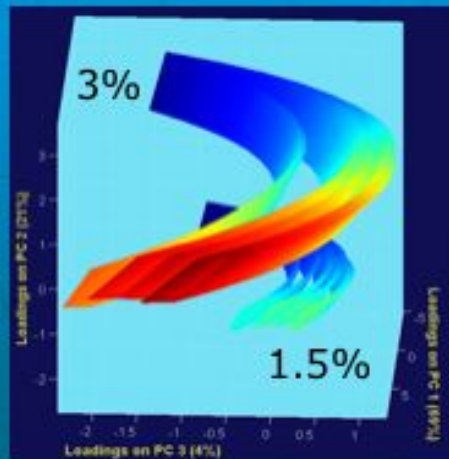


How to discern?

Clearer Picture



5 Reactors, 3%





Moving Toward Accurate Mercury Isotope Analysis: Evaluating Transport and Transformation Processes

Paul G. Koster van Groos, Nuclear Summer Science Internship Program (LLNL), University of California, Berkeley

James R. Hunt, Department of Civil and Environmental Engineering, University of California, Berkeley

Ross Williams, Chemical Biology and Nuclear Science Division, Chemistry and Materials Science Directorate, Lawrence Livermore National Laboratory

Brad K. Esser, Chemical Biology and Nuclear Science Division, Chemistry and Materials Science Directorate, Lawrence Livermore National Laboratory



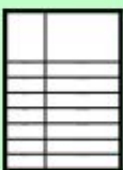
Two different sample introduction systems, an Aridus desolvating nebulizer and a PFA nebulizer with cyclonic spray chamber, in conjunction with a GV Instruments isotopic multi-collector inductively coupled plasma mass spectrometer (MC-ICP-MS), were evaluated for use in mercury isotope analysis. Results indicate that a significant fraction of mercury is lost within the desolvating nebulizer, and that both systems, albeit to differing degrees, suffer from mercury effects that could influence isotopic measurements. Our measurements indicate that two or more fractionating processes could be occurring within the sample introduction systems. We suggest that these include the disproportionation of mercurous (Hg_2^{2+}) ions, as well as diffusion-limited sorption of elemental mercury (Hg^0). Future experiments will seek to eliminate these fractionating processes within the analytical method by complexing mercuric (Hg^{2+}) ions with strong chelators. Other experiments should verify the degree to which the processes identified above fractionate mercury.

Introduction

Understanding of mercury transport and transformation processes is needed as the public attempts to reduce environmental exposures to mercury. These processes have proven difficult to quantify, but an examination of the seven stable mercury isotopes could provide significant insight.

The broad objective of my research is to experimentally determine how transport and transformation processes influence mercury isotope composition and to evaluate these processes by examining mercury isotope compositions of environmental samples, where only mercury fractionation indicates essential variations exist. Expectations are that many processes could be described by relatively simple Rayleigh fractionation and mixing models.

To enable this line of research, accurate and precise analytical methods are needed. This work describes initial efforts at quantifying mercury isotope composition using a MC-ICP-MS instrument.



Methods

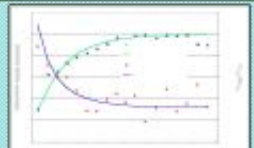
- We utilized two separate sample introduction systems leading to a GV Instruments isotopic MC-ICP-MS using one family type to analyze masses 196 to 200.
 - PFA Nebulizer with cyclonic spray chamber
 - An Aridus desolvating nebulizer
- Different concentrations of Mercury and Thallium in $2\% HNO_3$ were analyzed. The predominant species of mercury in these solutions is Hg_2^{2+} .
- Workset with dilute HNO_3 .




Results

Raw output intensities from the MC-ICP-MS instrument (19 + cycles) were evaluated, as well as raw $^{200}Hg/^{199}Hg$ ratios.

Average values for each sample introduction system. If isotropy using the Aridus system is 5% higher than using the cyclonic spray chamber, the intensity of the Hg signal relative to non-volatile Tl is 5% greater in the cyclonic spray chamber, indicating a potential loss of volatile Hg in the Aridus.

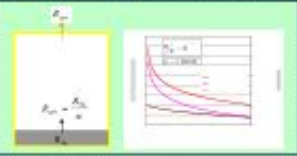


Discussion

- Changes in isotopic and average ratios observed during the course of sample runs and washes were placed in the context of known fractionation processes.
- Two potential isotope fractionating processes were evaluated using Rayleigh fractionation models.
 - Disproportionation of Hg_2^{2+} ions during nebulization
 - Diffusion-limited sorption of Hg^0 on various surfaces

Rayleigh Fractionation of Isotopes

Rayleigh fractionation models assume an open system where isotopes are transported or transformed at different rates and removed from the system steadily. Relative rates are described by α , the fractionation factor.



Environmental Context

- Mercury is a pollutant of concern that can severely affect the central nervous system.
- Large exposures can lead to crippling illness and potentially death.
- The primary exposure pathway for mercury is through the environmental production of methylmercury, which subsequently bioaccumulates in animal tissues.
- Two large and ongoing sources of mercury to San Francisco Bay result from mercury mining along the coastal range and gold mining in the Sierra Nevada.
- To reduce mercury contamination, it is important to identify the relative importance of different sources. Variations in isotopic composition could help.
- The identification of mercury sources using mercury isotope composition requires a precise and accurate measurement technique and an improved understanding of mercury fractionating mechanisms.




We hypothesize that historic mining activities (shown below) have led to mercury sources with distinct and identifiable isotopic compositions (indicated above) that may be traced through the environment.

Figure 1

Evaluation of ^{200}Hg isotopes (normalized by maximum signal at given concentration) and raw $^{200}Hg/^{199}Hg$ ratios using the Aridus sample introduction system. The $^{200}Hg/^{199}Hg$ ratios decrease with ^{200}Hg intensity increases towards an apparent steady state.

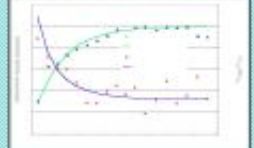


Figure 2

Evaluation of signal intensity and $^{200}Hg/^{199}Hg$ ratios during one complete run in both cyclonic spray chamber and Aridus systems. Hg signals display much greater 'noisiness' than Tl signals. $^{200}Hg/^{199}Hg$ ratios increase during washes.

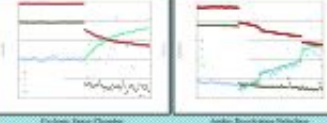
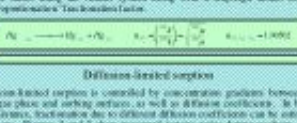
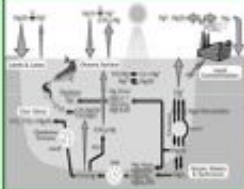


Figure 3

Rayleigh plot during sample washes in the Aridus system. Note the increase in $^{200}Hg/^{199}Hg$ ratios as the fractionation factor decreases.

The mercury cycle is complex, but different sources may have different isotopic compositions that can be traced throughout the cycle.



A mercury furnace and condensing system with major mercury sources identified and isotopic compositions estimated based on Rayleigh models. Data (R) values are referred to samples on New Almaden Mine.



During hydraulic mining for gold in the Sierra, large quantities of mercury were used in the slimes in the amalgamation process.

Conclusions

- Isotopic fractionation occurs with the two sample introduction systems utilized.
- Disproportionation and diffusion-limited sorption may be the fractionating processes that explain much of this behavior.
- The Aridus desolvating nebulizer has much greater sensitivity for non-volatile species than the PFA nebulizer with cyclonic spray chamber.
- Future work:
 - Complex Hg^{2+} species to prevent disproportionation and Hg^0 loss
 - Design experiments to examine disproportionation and diffusion-limited fractionation in greater detail



Compton-Electron Tracking Imaging Gamma-Ray Detector

Rion E. Graham, Nuclear Science Summer Internship Program



Glenn T. Seaborg Institute

Ron Wurtz, I-Division, PAT

ABSTRACT

We have developed a novel Compton imaging gamma-ray detector targeted at energies in the 2.6 MeV range. The current configuration consists of a 1024-by-1024 pixel intensified CCD camera coupled to a Terbium-doped-glass cubic fiber array. Measured photon-count characteristics of MIP tracks allow for predictions of spatial and energy resolutions of Compton electron events within the cube through a simple conversion of specific-energy loss. A detailed quantitative comparison between the system's native sampling resolution and the angular resolution of electron tracks is in progress.



- Andor ICCD Camera
- Face Plate/ Cube Fastener
- Reflective Mirror Insert w/ foam cushioning
- Nestled Fiber Cube

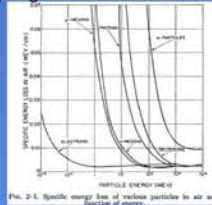
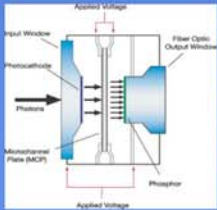


FIG. 2-1. Specific energy loss of various particles in air as a function of particle energy.

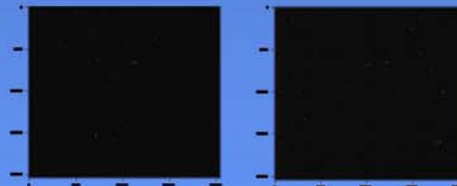
$$\frac{d_{MeV}}{cm} \Big|_{MIPS:glass} \times \left(\frac{\text{photons}}{cm} \Big|_{MIPS} \right)^{\Delta} \cos^2(\theta) = \ddot{a}$$

$$\frac{d_{MeV}(E)}{cm} \Big|_{electron:glass} \frac{d_{cm}}{e} = \frac{\text{photons}}{cm} = \text{spatial resolution}$$

Measured Spatial Resolution: $382 \cdot \cos(\theta)$ photon/cm, electron @ 1MeV
or $26/(\cos(\theta))$ $\mu\text{m}/\text{photon}$, electron @ 1MeV



The use of an intensified CCD allows for the detection of a single photon. In addition, the camera's 50% Q.E. value means that half of the photons coming from the intensifier will be measured. In contrast, the former cameras were not intensified and had a Q.E. of only about 10%, producing images like those to the right. The difference in track resolution and intensity in stunning.



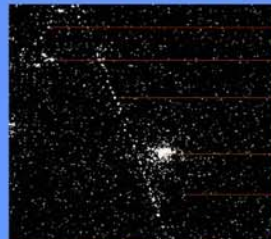
Future Work: Our first course of action is to purchase a second camera to be used in a coincidence-triggered simultaneous imaging configuration (similar to images seen on the left.) Once functional, we will be able to reconstruct continuous tracks for even greater energy and angular resolution. The correlation of the pictures will also help to further reduce noise and spurious events. Additionally, we hope to obtain a several-Mev gamma-ray source to produce electron tracks of sufficient length to test our predicted resolution.

The cubic fiber array (fibercube) is made of Tb-doped glass fibers, each $15\mu\text{m}$ in diameter, which are grouped into bundles 10 fibers high. These bundles are then joined to form '2-D' layers which are in turn stacked orthogonally to form the cube.



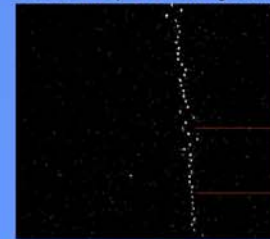
- Standard CCD light fall-off
- Fiber bundle separation
- Damaged Fiber layers

Image reduction is a vital step in the quantitative analysis of desired events. The bias, dark-current events, leaked visible photons, photocathode events, etc. must all be identified and numerically eliminated.



- High energy electron (in plane)
- Lower energy electron (out of plane)
- MIP track
- Photocathode event
- Spurious event (leaked photon, dark, etc)

The MIP track shown below is from a 10ms exposure. There is a balancing between probability of occurrence and non-MIP noise that determines the optimal exposure length. The back-end mirror helps to intensify only those events that are within the cube, providing additional help when distinguishing particle tracks.



- Non-linearity due to fibers' projection irregularity
- High density, well-resolved MIP track

This work was performed under the auspices of the U.S. Department of Energy by the University of California Lawrence Livermore National Laboratory under contract No. W-7405-Eng-48.



Contextually-Aware Expert-System for Automated Nuclear Threat Assessment

Shadi Z. Ghayeb, Rensselaer Polytechnic Institute,

S. Labov, M. Pivovarov I-Division, Physics & Advanced Technologies Directorate
Lawrence Livermore National Laboratory,



Glenn T. Seaborg Institute



The detection of a nuclear or radiological device in the United States would have a catastrophic effect. These national laboratories, universities, industries and research centers have been collaborating in finding solutions to the issues of dealing with countering clandestinely delivered nuclear and radiological threats. Current detection monitors deployed at border-crossings and other strategic locations are still susceptible to high false-alarm rates, due to the detection of radioactive nuisance sources from industrial, medical or naturally occurring radioactive material (NORM). High false alarms limit the monitors' effectiveness at the screening of cargo, trucks and personal vehicles. Our goal is to develop a detailed categorization system called, "Contextually-Aware Expert-System for Automated Threat Assessment" for guiding the accuracy of an instrument's identification. The system involves a program that captures the deep knowledge and understanding possessed by a human expert, and based on particular observables, returns a specific answer or response that fits the data. This system will be provided as effective support of the field agents so that they can process an order of magnitude more events per unit time while halving the number of calls to the primary reach-backs.

Introduction:

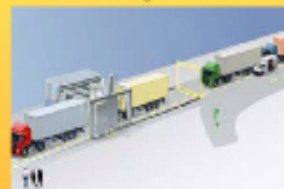
This project combines ambiguous output collected from border-crossing detectors with contextual information in a novel expert system to help resolve radiation alarms.

In the instance of such an alarm, a human expert is often required to intervene to resolve the situation. The expert considers the spectroscopic signal while incorporating contextual information and past experience in similar situations to make a determination to pass the shipment or initiate a detailed search. This project will develop a computerized system that captures the deep knowledge and understanding possessed by a human expert where the project returns a specific answer or response to fit that data.

Radiation Portal Monitor (RPM)



Traffic through RPM



Methods:

As part of my role in this project I will perform a mapping of the natural radiation background. A BNC SAM-935 detector system was mobilized into a backpack unit. Sensor data is sent to a hand-held palm device and transmitted to a remote database for storage. Included in the transmission are time of fix, GPS coordinates, count rate, and spectrum information. This technique of measuring radiation levels and analyzing the collected spectrum will be familiar to the secondary inspections of cargo performed by border patrol custom agents.

In analyzing the collected spectrum, artificial intelligence will be used to provide information about the manifest to implement into our system.



Results:

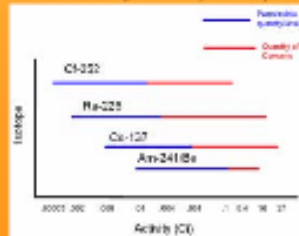
We have begun assembling databases on commonly used nuclear material. In addition to the many analysis of nuisance sources we have collected, we are collecting lists of manufacturers, users and shippers of nuclear materials. This includes information about possible applications for each isotope in commercial and medical uses. These data will provide inputs to the user and the expert system regarding the normal use of these materials, and will help in the anomaly detection analysis.

Cs-137 Spectrum



Spectrum analysis identifies isotope

Permissible and dangerous activity levels for portable gauges



Expert system determines the threat level

Discussion:

In the instance of such an alarm, a human expert is often required to intervene to resolve the situation. Our plan is to refine our system towards our eventual goal of implementing a fully-automated system to support the Advanced Spectroscopic Portal monitors in the field. This requires a combination of a deep understanding of a specific problem and a hierarchical series of rules.

We anticipate the impact of our system will be most significant when the number of measurement systems increases as more points of entry, state and local detection systems are implemented. The number of measurement systems could easily increase by factors of 10 or more, which would overwhelm the current primary reach-back capabilities.

This work was performed under the auspices of the U.S. Department of Energy by University of California Lawrence Livermore National Laboratory under contract No. W-7405-Eng-48.

UCRL-60500-01



Monitoring Nuclear Reactors with Antineutrinos



Alex Johnson, Nuclear Science Summer Internship Program

Adam Bernstein, I Division, PAT Directorate



Glenn T. Seaborg Institute

Theory

- Antineutrino Production¹
- Detection²
 - High flux of antineutrinos
 - Scintillator volume
 - Advanced shielding
- Preventing Diversion
 - Detecting an abnormal antineutrino rate
 - Modeling probable diversion schemes

Experiment

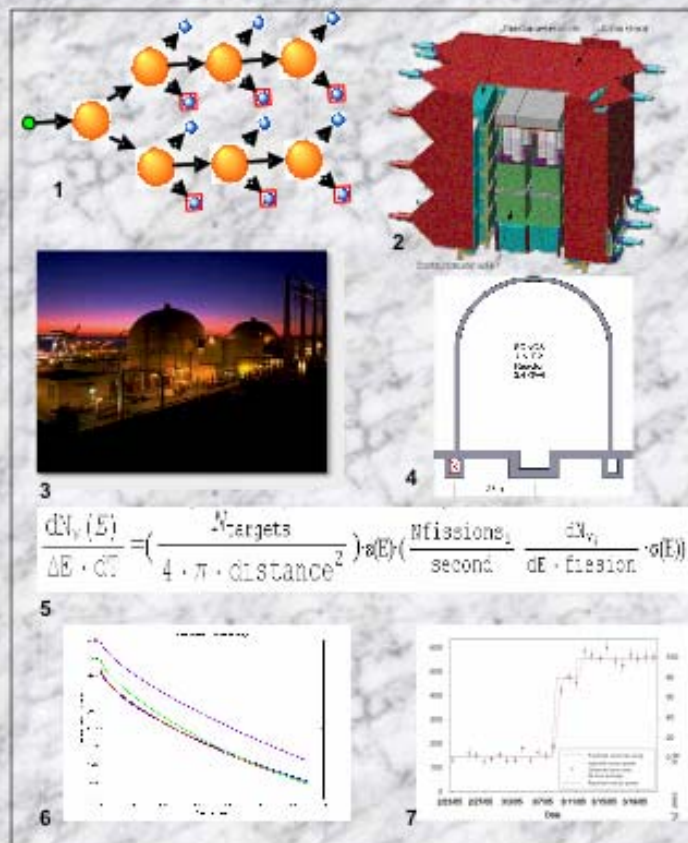
- SONGS³
 - Operated for 1.5 years with little or no maintenance
 - Located 25 meters from reactor core⁴

Simulation

- Diversion Scenarios
 - Baseline - Standard reactor cycle
 - A - 3.5% replaced with 1.5%
 - C - Spent fuel replaced with fresh fuel
 - D - Reactor run at 105% power
- ORIGEN
 - Provides burnup dependent isotopic data for each scenario
 - Predicts fission rates for each isotope per burnup step
- Conversion⁵

Conclusions

- Due to uncertainty in simulation A and C are undetectable⁶
- Diversion D is different from the baseline by 5%
- Diversion D verifies methods and supports use in power monitoring
- Can monitor power weekly to within 3%⁷





Glenn T. Seaborg Institute

Improving Compton Imaging through Signal Decomposition

Nathanael Kuo^{1,3}, Undergraduate Summer Institute
Dan Chivers², Dr. Kai Vetter¹

¹ Lawrence Livermore National Laboratory
² University of California, Berkeley
³ University of Illinois at Urbana-Champaign



ABSTRACT

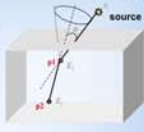
In order to get efficient results for Compton Imagers, we developed a new method for calculating the positions and energies of gamma ray interactions. This method decomposes double-sided strip detector (DSSD) signals through the implementation of singular value decomposition (SVD) not only provides an alternative method of calculating positions and energies, but may also transcend existing methods by making full use of composite signals normally thrown out by other methods. As a result, the efficiency of Compton Imagers can be greatly improved upon successful implementation of signal decomposition.

INTRODUCTION

Gamma ray detectors today have reached a point in their technology where they can determine gamma radiation energies with great precision and efficiency. However, with the many nuclear threats around the world, there has grown a need not only to detect gamma rays but also to see where the radiation is coming from. As a result, Compton imaging is a developing technique that images localized radiation sources by superimposing back-projecting cones determined by the angles between interactions due to Compton scattering.

$$\cos(\theta) = 1 - m_e c^2 \left[\frac{E_1}{E_1 + E_2} \right]$$

Compton scattering is caused when a gamma ray ricochets, leaving some energy behind.



Compton Imaging uses the positions of interactions to back-project a cone of possible source locations

The exact location of the source can be determined by finding the intersection of the back-projecting cones



However, accurate Compton imaging requires solid and efficient methods to extract the position and energy information of each interaction from the detector signals. Consequently, we propose to improve the current method of position calculation in double-sided strip detectors (DSSD) by using singular value decomposition (SVD) to decompose the detector signals. This method would be a new robust way of calculating positions as well as a step towards making use of many signals often ignored in other position calculation methods.

METHOD

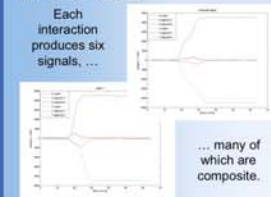
First, we took measurements from a high-purity Germanium (HPGe) DSSD, where gamma rays were collimated to a fan beam centered on one of the electrode strips. We then saved all the produced signals (six for each interaction) in order to test the accuracy of the SVD in measuring the position of each interaction.



A picture of the HPGe double-sided strip detector



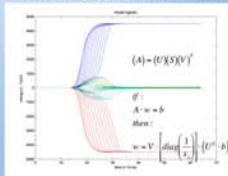
Each interaction produces six signals, ...
... many of which are composite.
Most existing methods for position determination involve calculating time differences between these signals. However, they have a significant drawback in that many signals which result from very close interactions (known as composite signals) cannot be used in Compton imaging.



In theory, signal decomposition would help recover information from these composite signals. Therefore, we generated several model signals using a finite-element mesh model to create a system response matrix for the SVD. Execution of the signal decomposition equations then resulted in weight vectors, from which we can interpolate the position of the interaction by taking a weighted average. As a result, the SVD method should not only produce accurate position calculations for more interactions, but also give an indication of the depth of our understanding of the physics in the detector.

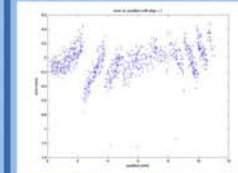


The model signals were created using a finite-element mesh model



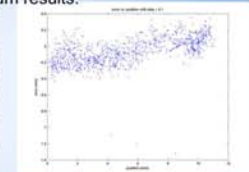
Each set of data signals can be interpreted as a linear combination of several model signals through signal decomposition

RESULTS



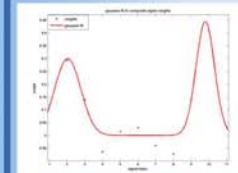
Step sizes that were too large created striations in the results.

When we implemented the signal decomposition, we compared the results to that of the benchmark method used for non-composite signals. We encountered a problem on the way, however, since the model and data signals were not centered. We thus applied an iterative approach to centering the signals, adjusting the step size for optimum results.



Signal decomposition demonstrated relatively small errors when centered

Once we corrected for step size, the results showed an encouraging small error. This error was within hundreds of microns, approximately the magnitude of the inherent uncertainty due to charge cloud size. The results have a slight slope, however, which may be due to model signal errors. Nonetheless, they show that SVD works well for non-composite signals.



A Gaussian fit showed two distinct peaks where the interactions occurred

Signal decomposition also worked fairly well for composite signals. There were no other methods to compare our work, but the results show that SVD is able to distinguish between two close interactions. A fit of a linear combination of Gaussian functions clearly denotes the two interactions where these particular composite signals originated.

CONCLUSION

Through this experiment, it is clear that signal decomposition is an exciting and promising new approach to Compton imaging. Since our work was preliminary, results are only bound to improve upon further research and study. Much needs to be done, however, including the generation of model signals applied to more signal energies and position dimensions. Nonetheless, each step will provide greater precision and accuracy to the growing world of Compton Imagers.

Summer students at LLNL 2006

